Initial Clinical Investigation of [^{18}F]Tetrafluoroborate PET/CT in Comparison to [^{124}I]Iodine PET/CT for Imaging Thyroid Cancer

Samuel Samnick, PhD, Ehab Al-Momani, PhD,* Jan-Stefan Schmid, MD,* Anja Mottok, MD,† Andreas K. Buck, MD,* and Constantin Lapa, MD**

Aim: Recently, [^{18}F]tetrafluoroborate ([^{18}F]TFB) has been introduced as a versatile PET probe for imaging the human sodium/iodide symporter activity. This pilot study aimed to compare [^{18}F]TFB-PET/CT with [^{124}I]NaI-PET/CT imaging in thyroid cancer patients.

Methods: Nine patients with newly diagnosed differentiated thyroid cancer underwent both [^{18}F]TFB- and [^{124}I]NaI-PET/CT after total thyroidectomy. PET/CT scans were visually analyzed for the presence of remnant thyroid tissue and for metastatic lesions on a patient and lesion basis. For semiquantitative analysis, thyroid remnant/tumor to blood pool ratios were calculated.

Results: All patients presented with positive [^{18}F]TFB and [^{124}I]NaI-PET/CT scans. Retention of ^{124}I in remnant thyroid tissue was significantly higher as compared with [^{18}F]TFB ($P < 0.01$). In a lesion-based analysis, both tracers identified an almost equal number of foci with [^{18}F]TFB depicting a total of 41 foci and ^{124}I a total of 40 foci, respectively. In 6 of 9 patients, both radiopharmaceuticals returned an identical number of foci. Two ^{124}I-positive benign thyroid remnants were missed by [^{18}F]TFB-PET/CT in a single patient. In another case, both tracers identified different thyroid remnant tissues in the cervical region. Notably, [^{18}F]TFB demonstrated additional (^{124}I-negative) cervical lymph node metastases in 2 patients, leading to an overall agreement between the radiotracers of 91% (74/81 foci).

Discussion: In this pilot study, [^{18}F]TFB-PET was not inferior to [^{124}I]NaI-PET for detecting thyroid cancer and its metastases and was able to detect [^{124}I]NaI-PET-negative viable differentiated thyroid cancer metastases. Further clinical evaluation as a PET tracer for imaging thyroid pathophysiology and human sodium/iodide symporter expressing neoplasms is highly warranted.

Although planar (whole-body) scintigraphy and single photon emission computed tomography targeting of the human sodium/iodide symporter (hNIS) with radioiodine (^{123}I and ^{131}I) or sodium [^{99m}Tc]pertechnetate ([^{99m}Tc]TcO_4^-) for the management of benign and malignant thyroid diseases has been performed for more than 70 years,[1,2] current alternative options for PET imaging of hNIS expression are still very limited. Sodium [^{124}I]iodide ([^{124}I]NaI), the only available diagnostic radiotracer suitable for PET imaging, has proven its diagnostic superiority over [^{99m}Tc]pertechnetate- and radioiodine-based scintigraphy.[3–5] However, [^{124}I]iodide has several disadvantages that prevent routine diagnostic use, including poor physical characteristics (eg, positron yield of only 23% compared with 97% for ^{18}F), comparably high effective patient doses or the need for late imaging with optimal target-to-background ratios after 24 hours.[6,7] Moreover, its availability is limited and its production relatively complex.[8,9] Clinically, [^{124}I]NaI-PET has been mostly used for dosimetric purposes.[10–12] As a potentially beneficial alternative, ^{18}F-labeled tetrafluoroborate ([^{18}F]TFB) was recently introduced and evaluated in a pilot human dosimetry study in 5 patients.[13] The aim of this pilot study was to provide first evidence on the diagnostic performance of [^{18}F]TFB-PET/CT in patients with newly diagnosed thyroid cancer in comparison to [^{124}I]NaI-PET/CT.

METHODS

[^{18}F]TFB was administered in compliance with §37 of the Declaration of Helsinki and The German Medicinal Products Act, AMG §13 2b and in accordance with the responsible regulatory body (Regierung von Oberfranken, Bavaria, Germany). All subjects gave written informed consent before imaging.

Subjects

Nine patients (2 male and 7 female subjects; age, 45 ± 12 years; range, 26–56 years) with newly diagnosed differentiated thyroid cancer were included. All patients had undergone total thyroidectomy and presented before radioiodine remnant ablation. Thyroid-stimulating hormone (TSH) levels, as measured at the day of [^{18}F]TFB injection, were endogenously stimulated with levels between 18.8 and 125.0 IU/mL in all but one case (patient 5 presenting only 17 days after total thyroidectomy). Patient 8 presented with endogenously suppressed TSH levels because of thyroid hormone secretion by extensive tumor burden. Iodine contamination was excluded by urine testing in all patients. Detailed patient characteristics are given in Table 1.

Preparation of Sodium [^{124}I]iodide ([^{124}I]NaI) and [^{18}F]Fluorotetrafluoroborate ([^{18}F]TFB)

Preparation of [^{124}I]NaI

Sodium [^{124}I]iodide was produced in-house by a ^{124}Te(P, n)^{124}I reaction on a 16.5 MeV PETtrace cyclotron (GE, Uppsala, Sweden). Irradiation was performed with a preprepared solid target consisting of [^{124}Te]TeO_2 (95%) and Al_2O_3. After irradiation at the cyclotron, the shuttle was transferred fully automatically via a tube system to the ALECO Halogen 2.0 extraction module (Comecer SpA, Castel Bolognese, Italy). Extraction was performed by heating the shuttle and trapping of the vaporized [^{124}I]iodide, followed by elution of [^{124}I]iodide in the form of sodium [^{124}I]iodide with a 0.05 N NaOH solution. The extracted [^{124}I]NaI was buffered with PBS and sterile-filtered through a 0.22 μm filter

TABLE 1. Patient Characteristics

No.	Age	Sex	Disease	TNM	TSH (IU/mL)	hTg (ng/mL)	Recovery (%, 70–130)	hTg Antibodies (IU/mL, 0–100)
1	56	F	PTC	pT1b, pN0 (0/4), Mx	55.1	2.2	100	16
2	51	M	PTC	pT3, pNx, Mx	66.7	4.2	101	20
3	40	F	PTC	pT1b, pNx, Mx	47.9	7.3	99	3
4	44	F	PTC	pT1a(m), pNx, Mx	52.6	0.3	101	28
5	55	F	PTC	pT1a, pN0 (0/1), Mx	18.8	21.4	101	28
6	51	F	PTC	pT1a, pNx, Mx	27.8	0.7	80	992
7	26	F	PTC	pT2(m), pN1a (9/22), Mx	125.0	<0.2	84	560
8	55	F	FTC	pTx, pNx, cM1	<0.01	28,760	100	96
9	28	M	FTC	pT2, pNx, Mx	68.9	81.5	95	22

F indicates female; FTC, follicular thyroid cancer; hTg, human thyroglobulin (measured in serum); M, male; PTC, papillary thyroid cancer.

(Millipore, Cork, Ireland) into a sterile vial for for clinical applications. Further details on the production of sodium [^{124}I]iodide using the Comecer ALECO Halogen 2.0 module has been described previously elsewhere.[14]

Preparation of [^{18}F]TFB

[^{18}F]TFB was prepared in analogy to the method described previously by Jauregui-Osoro et al with some modifications, using a Raytest SynChrom module (Raytest, Straubenhardt, Germany).[15] Briefly, [^{18}F]fluoride (typically 15-20 GBq) produced via a proton-irradiation of [^{18}O]water (97 atom %; ABX, Radeberg, Germany) on a 16.5 MeV GE-PETtrace cyclotron (GE Healthcare, Uppsala Sweden) with a beam current of 50 μA and an irradiation time of 10 to 15 minutes, was trapped in a QMA cartridge (Sep-Pak Light QMA cartridge; Waters, Eschborn, Germany). The QMA cartridge was conditioned with 1.0 M sodium hydrogen carbonate (10 mL) followed by water for injections (10 mL) and air. Hydrochloric acid (1.5 M, 1.2 mL) was then passed through the QMA cartridge, eluting the [^{18}F]F$^-$ into the reactor containing 1 mg of $NaBF_4$ (Sigma-Aldrich, Sulzbach, Germany) in 0.1 mL water. The reaction mixture was heated to 60 °C for 20 minutes, cooled to room temperature and passed through a silver ion-loaded cation exchange cartridge (OnGuard II AG; Dionex, Sunnyvale, CA), to remove chloride and raise the pH, and through 2 alumina columns (Sep-Pak Light Alumina N; Waters) to remove unreacted [^{18}F]fluoride. The OnGuard II AG-cartridge and the Sep-Pak Light Alumina N-cartridges were conditioned with 10 mL of Ultrapure Water (Merck, Darmstadt, Germany) and 10 mL Ultrapure Water/5 mL air, respectively, and assembled before use. Purified [^{18}F]TFB was collected in a glass flask, diluted with water for injection (aqua ad iniectabilia), and sterile filtered through a 0.22 μm sterile filter (Millipore, Cork, Ireland) into a sterile vial (IBA, Berlin, Germany). The [^{18}F]TFB solution was subjected to quality control consisting of HPLC and radio-TLC analysis for radiochemical purity, LAL for pyrogen, and test for sterility before intravenous administration to patients. Radiochemical purity was greater than 99%, and the injection solution of [^{18}F]TFB was sterile and pyrogen-free.

PET Imaging

Imaging was performed on a dedicated PET/CT scanner (Siemens Biograph mCT 64; Siemens Medical Solutions, Erlangen, Germany) with a time interval between both PET scans of 2 days in all cases. Image acquisition was started 40 minutes after injection of 276 to 375 MBq (median, 300 MBq) of [^{18}F]TFB. ^{124}I scans were performed 24 hours after oral application of 21 to 38 MBq (median, 30 MBq) of [^{124}I]NaI. Corresponding low-dose CT scans for attenuation correction were acquired from skull to proximal thighs. Consecutively, PET emission data were acquired in 3-dimensional mode with a 200 × 200 matrix with 2 to 3 minutes ([^{18}F]TFB) or 3 to 5 minutes of (^{124}I) emission time per bed position, respectively. After decay and scatter correction, PET data were reconstructed iteratively with attenuation correction using dedicated software (Siemens Esoft; Siemens, Erlangen, Germany).

Image Analysis

First, all scans were visually analyzed by 2 experienced nuclear medicine specialists (J.-S.S. and C.L.). PET-positive lesions were determined as focally increased tracer retention as compared with surrounding normal tissue or contralateral normal structures. Analysis was performed according to previous studies.[16,17] Briefly, PET-positive foci within the thyroid bed were classified as thyroid remnant tissue, a focus outside the thyroid bed of iodine uptake was classified as metastatic tissue. Lesion- and patient-based analyses were performed to assess the diagnostic performance of [^{18}F]TFB and [^{124}I]NaI PET/CT.

The lesion-based analysis counted the total number of PET-positive foci; the patient-based analysis counted the number of PET-positive subjects. The level of agreement regarding concordantly detected foci was determined.

For semi-quantitative analysis, volumes of interest were placed over the areas with increased tracer uptake. Using autocontouring, these volumes of interest (with a minimum volume of 1 cm^3) were used to derive maximum (SUV_{max}) and mean (SUV_{mean}) standardized uptake values. For background reference, bloodpool SUV_{max} and SUV_{mean} were also derived. Therefore, 2D regions of interest (ROIs) with a diameter of 25 mm were drawn in the left ventricular cavity. Thyroid/tumor-to-background ratios (TBR) were calculated for both SUV_{max} and SUV_{mean}. A maximum of up to 3 TBR per location (local thyroid bed, lymph nodes [LNs], and distant metastases) were analyzed.

Statistical Analysis

Most of the data presented are descriptive. Statistical analyses were performed using PASW Statistics software (version 22.0; SPSS, Inc. Chicago, IL). Quantitative values were expressed as median and interquartile range (IQR) as appropriate. Wilcoxon signed rank test was used to examine differences between agents.

RESULTS

Clinical

Seven patients presented with newly diagnosed papillary thyroid cancer, the remaining 2 with follicular TC. One patient with

TABLE 2. Detection of Local Thyroid Remnants, LN, and Distant Metastases for Both [^{18}F]TFB- and [^{124}I]NaI-PET/CT

		[^{18}F]TFB			[^{124}I]NaI		
No.	**More Lesions Detected Using**	**Thyroid Bed**	**LN**	**Distant Metastases**	**Thyroid Bed**	**LN**	**Distant Metastases**
1	^{124}I	3	0	0	5	0	0
2	Comparable	4	0	0	4	0	0
3	Comparable	2	0	0	2	0	0
4	Comparable	3	0	0	3	0	0
5	Comparable	2	0	0	2	0	0
6	Comparable	3	0	0	3	0	0
7	[^{18}F]TFB	1	2	0	1	0	0
8	Complimentary	1 (different from ^{124}I)	1	12 lung + 6 bone	1 (different from [^{18}F]TFB)	0	12 lung + 6 bone
9	Comparable	1	0	0	1	0	0

FTC (patient 8) was referred with the suspicion of metastatic disease due to serum thyroglobulin levels greater than 20,000 ng/mL. Another patient (patient 7) with PTC presented after total thyroidectomy (pT2m) disease with the largest tumor diameter of 15 mm and resection of 9 LN metastases (of a total of 22 LN) in the central cervical compartment. Upon presentation at the thyroid outpatient unit, serum thyroglobulin levels were not detectable (<0.2 ng/mL) with potential interference by elevated thyroglobulin antibodies (560 IU/mL). Cervical ultrasound raised the concern for additional disease in left cervical LNs. For further workup, PET/CT was scheduled.

All other patients had no known extrathyroidal tumor spread. Patient characteristics are summarized in Table 1.

Imaging Results

Patient-Based Analysis

Both [^{18}F]TFB and [^{124}I]NaI-PET/CT detected positive lesions in all patients. PET-positive foci in the thyroid bed or along the thyroglossal duct qualified as benign thyroid remnants- were present in all patients. Both tracers additionally identified metastatic disease (lung and bone) in patient 8, whereas [^{18}F]TFB-PET exclusively depicted LN metastases in patient 7.

Lesion-Based Analysis

In a lesion-based analysis, the combination of both tracers identified a total of 42 lesions. [^{18}F]TFB-PET/CT returned 41 foci,

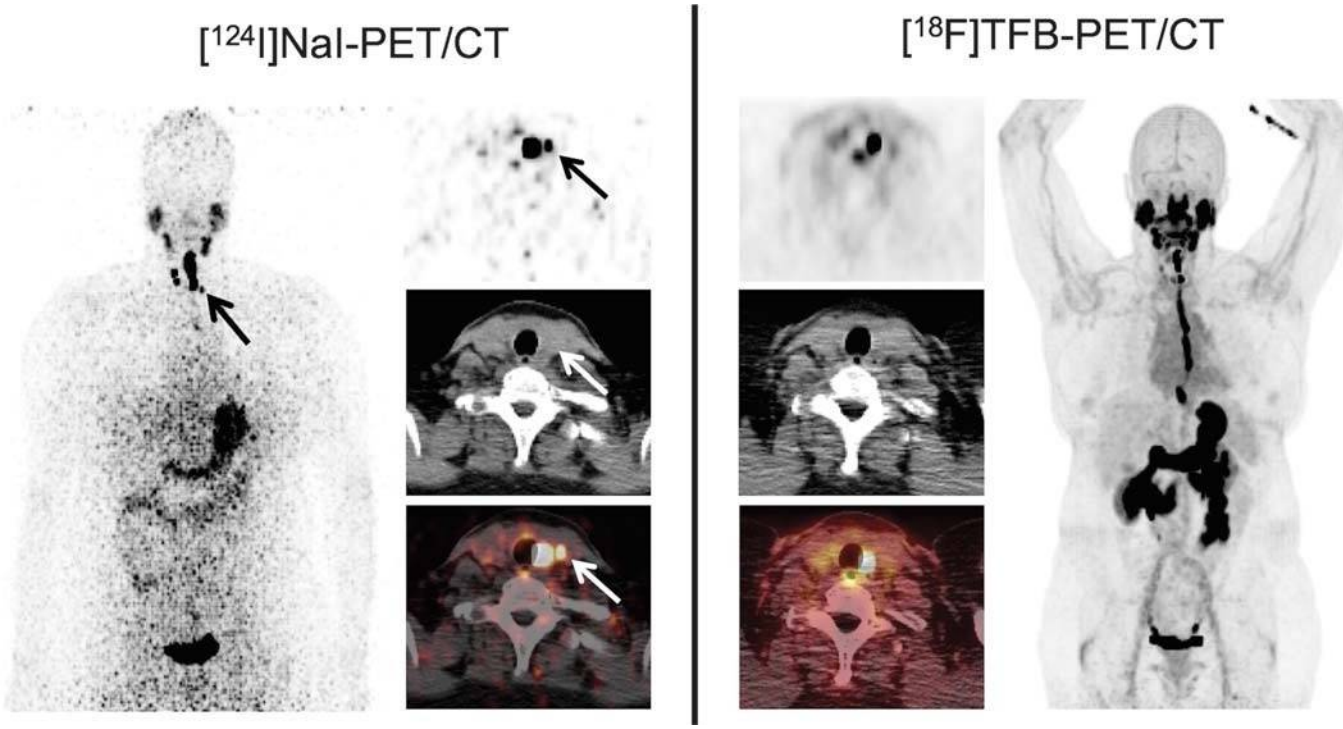

FIGURE 1. Comparison local thyroid remnant detection by [^{18}F]TFB- and [^{124}I]NaI-PET/CT. Display of maximum intensity projections (MIP; outer columns) and transaxial PET and combined PET/CT slices (inner columns). The 56-year-old patient (patient 1) with PTC presented after total thyroidectomy (pT1b). [^{124}I]NaI- and [^{18}F]TFB-PET/CT revealed remnant benign thyroid tissue in the thyroid bed and along the thyroglossal duct with 2 foci of remnant tissue missed by [^{18}F]TFB (arrows). No lesions suspicious for malignancy were detected.

with 20 foci being considered benign thyroid remnant tissue and the remaining 21 lesions as metastatic disease (3 LNs, 12 lungs, 6 bone). In comparison, 40 [^{124}I]NaI-PET-positive foci could be assigned to 22 benign foci and 18 metastases, respectively (12 lung, 6 bone). Individual results are shown in Table 2. In 6 of 9 subjects, both radiopharmaceuticals yielded an identical number of lesions. Two thyroid remnant lesions (as revealed by [^{124}I]NaI-PET) were missed by [^{18}F]TFB in patient 1 (Fig. 1), patient 8, both radiopharmaceuticals visualized different thyroid remnant tissues. In patients 7 and 8, LN metastases were only depicted using [^{18}F]TFB-PET/CT (Fig. 2). The level of agreement between both PET tracers was 74/81 (91%).

Thyroid-to-background ratios were significantly higher for [^{124}I]NaI as compared with [^{18}F]TFB (TBR_{mean} median/IQR, 186.2/62.4 versus 8.2/3.3 [$P < 0.01$]; TBR_{max} median/IQR, 303.4/553.8 versus 36.7/11.3 [$P < 0.01$]). In contrast, TBR_{max} derived from bone metastases in patient 8 were higher for [^{18}F]TFB as compared with [^{124}I]NaI (124.3 for [^{18}F]TFB versus 36.3 for [^{124}I]NaI; TBR_{mean}, 25.7 for [^{18}F]TFB versus 28.6 for [^{124}I]NaI; Fig. 3, Supplementary Table 1, http://links.lww.com/CNM/A108). For the LN metastases in patients 7 and 8 exclusively detected by [^{18}F]TFB, TBR_{mean} of 2.4 ± 0.0 and TBR_{max} of 3.2 ± 0.2 could be recorded. Individual patient data are provided in Supplementary Table 1, http://links.lww.com/CNM/A108.

DISCUSSION

The current options for hNIS imaging with PET are limited. Because of several physical and radiochemical drawbacks of ^{124}I as compared with ^{18}F, the ideal PET radiotracer for imaging hNIS would be labeled by ^{18}F, as ^{18}F is readily available and has a shorter half-life (110 minutes) compatible with typical imaging times and a low-energy (E_{max} = 0.634 MeV), high yield (97%) positron emission. This, among other reasons, advocates for a clinical evaluation of the newly described ^{18}F-labeled tracer [^{18}F]TFB as PET imaging probe for hNIS-expression.

[^{18}F]TFB was recently introduced in a preliminary human dosimetry study.[13] However, this pilot study represents—to the best of our knowledge—the first direct comparison of [^{18}F]TFB and [^{124}I]NaI in a cohort of newly diagnosed differentiated thyroid cancer patients. Our data show in general that [^{18}F]TFB-PET/CT is not inferior to [^{124}I]NaI-PET/CT. Both radiotracers were positive in all patients and yielded an identical number of foci in 6 of 9 patients. On a lesion basis, overall agreement was very high with 91% of concordant foci.

Interestingly, some differences between both tracers could be recorded. Whereas benign thyroid remnant tissue could be more readily visualized by ^{124}I both quantitatively and qualitatively with significantly higher TBR, DTC metastases demonstrated a

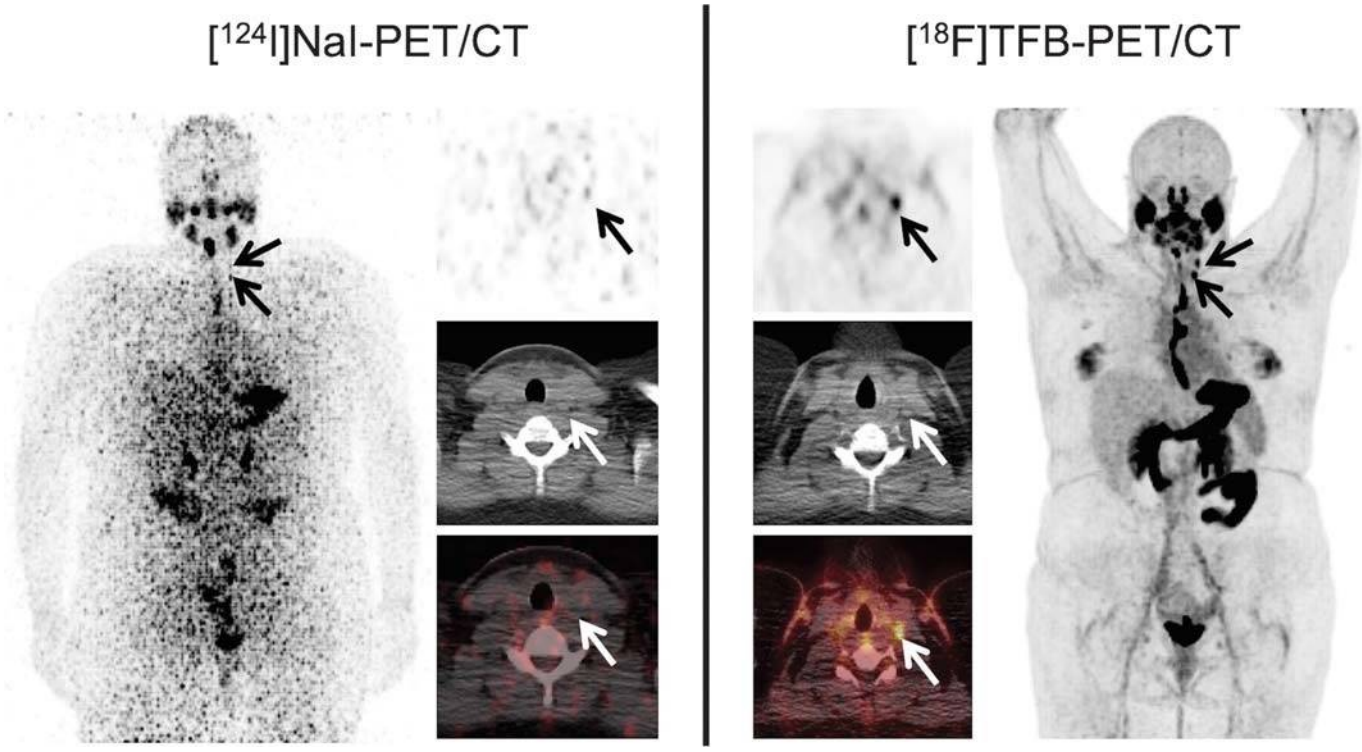

FIGURE 2. Example of a patient with PTC with LN metastases exclusively detected using [^{18}F]TFB-PET/CT. Display of maximum intensity projections (MIP; outer columns) and transaxial PET and combined PET/CT slices (inner columns). The 26-year-old patient (patient 7) with PTC presented after total thyroidectomy (pT2(m) disease with the largest tumor diameter of 15 mm) and resection of 9 LN metastases in the central cervical compartment (9/22 LN removed). Upon presentation at the thyroid outpatient clinic, serum thyroglobulin levels were not detectable (<0.2 ng/mL) with potential interference by elevated thyroglobulin antibodies (560 IU/mL). Cervical ultrasound raised the concern for additional disease in left cervical LNs. For further workup, PET/CT was scheduled. Beside a local thyroid remnant, [^{18}F]TFB-PET/CT confirmed ultrasound results by revealing 2 cervical LNs in the left lateral compartment with focally increased uptake, consistent with metastatic disease (arrows). In contrast, [^{124}I]NaI-PET was unremarkable for malignancy. Because of the discrepant findings, left lateral LN dissection was performed and yielded 6 additional cervical (micro-)metastases.

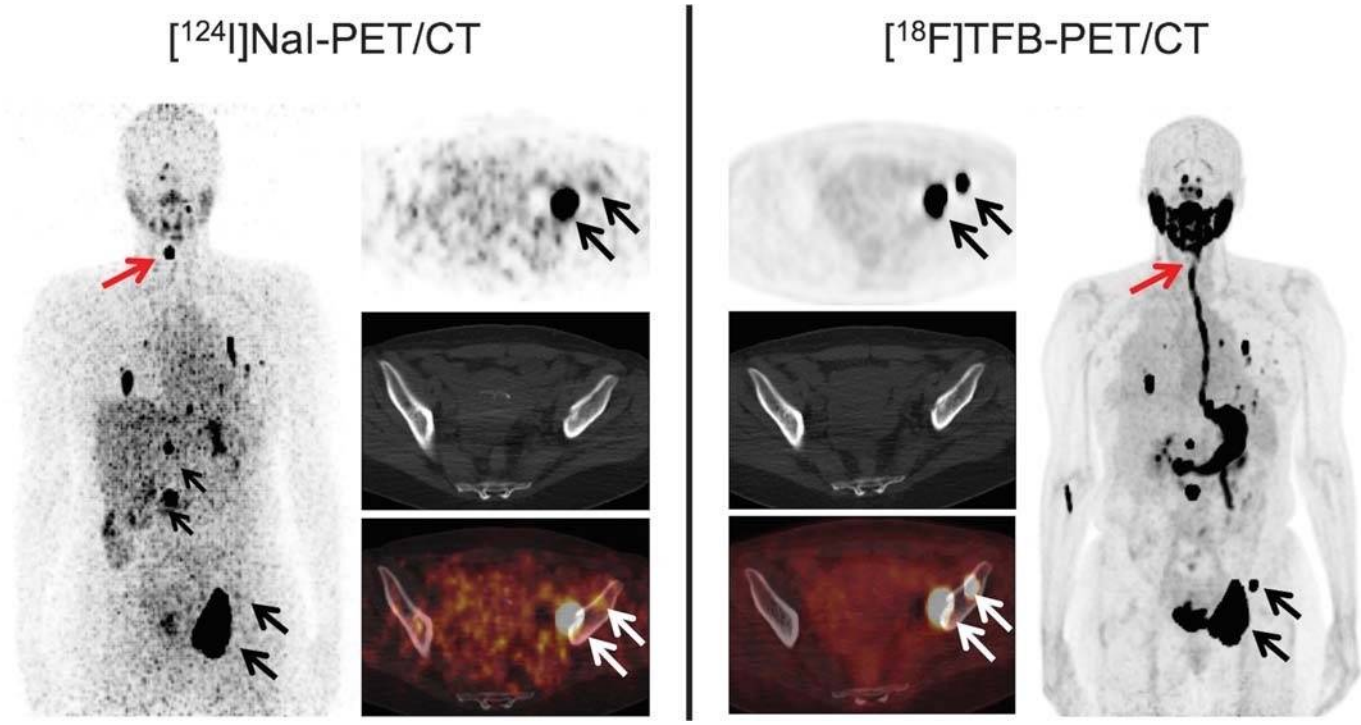

FIGURE 3. Complimentary information by [^{18}F]TFB- and [^{124}I]NaI-PET/CT in a patient with metastasized FTC. Display of maximum intensity projections (MIP; outer columns) and transaxial PET and combined PET/CT slices (inner columns). A 55-year-old patient (patient 8) with highly elevated serum thyroglobulin levels (>20,000 mg/mL) but no confirmation of thyroid cancer in the total thyroidectomy specimen was referred for further workup. Imaging with both tracers revealed multiple bone and lung metastases which partially presented with higher tumor–to–blood pool ratios in [^{18}F]TFB-PET/CT (black arrows). Thyroid remnant tissue was more readily visualized using [^{124}I]NaI-PET (red arrows; another small remnant exclusively detected using [^{18}F]TFB not shown).

relatively higher [^{18}F]TFB accumulation. Notably, histologically confirmed LN metastases in patient 7 were exclusively identified using [^{18}F]TFB-PET/CT. As both tracers are exclusively transported via hNIS, this finding cannot be fully explained yet. One explanation could be that in contrast to [^{124}I]iodide, [^{18}F]TFB -similar to [^{99m}Tc]pertechnetate- is considered a nonorganified hNIS ligand[8] and might detect lesions that have lost the ability to organify and, in consequence, accumulate iodine over a longer time. Potentially, the different time points of respective PET image acquisition, with [^{18}F]TFB scans starting 40 minutes after intravenous injection and [^{124}I]NaI scans being acquired 24 hours after oral administration, can account for at least part of the differences encountered, also with reference to the different count statistics of the 2 radioisotopes used. Although no firm conclusion can be drawn at this time point, the current results might suggest a potential advantage of [^{18}F]TFB over ^{124}I in malignant thyroid disease, especially in iodine-refractory cancers. Future research investigating the underlying biological pathways and implications as well as potential differences between benign and malignant thyroid tissue regarding [^{18}F]TFB is highly warranted.

Importantly, [^{18}F]TFB showed a biodistribution similar to [^{124}I]NaI in whole-body PET (Figs. 1–3), with a relatively high accumulation of [^{18}F]TFB in stomach and a rapid renal clearance, which parallels the known behavior of [^{99m}Tc]pertechnetate, another nonorganified hNIS tracer. The lack of radioactivity uptake in bone and joints confirms that [^{18}F]fluoride was not released in vivo after intravenous administration of [^{18}F]TFB. These pharmacokinetic attributes appear ideal for PET imaging, providing a good match with the half-life of ^{18}F.

This study has some limitations. First, it only comprises a low number of patients with only 2 of 9 presenting with metastatic disease. Second, no early [^{124}I]NaI-PET/CT imaging 4 hours after [^{124}I]NaI application was performed, and consequently, peak iodine uptake in thyroid and thyroid cancer tissue might have been missed. Additionally, the PET signal at later time points might also be influenced by the iodine retention status of the tissue. However, late imaging after 24 hours has been demonstrated to provide optimal target-to-background ratios[4] and was therefore chosen for this study.

In conclusion, [^{18}F]TFB-PET and [^{124}I]NaI-PET yielded comparable results clinically. Given the advantages of ^{18}F labeling and a potential benefit in thyroid cancer metastases, [^{18}F]TFB-PET might become a useful tool for assessing hNIS expression in human pathologies.

ACKNOWLEDGMENTS

The authors thank Simone Seifert, Elena Sotnikova, Eva Muffert, and Michael Schulze-Glück (members of the nuclear medicine PET team) for the support and assistance.

REFERENCES

1. Seidlin SM, Marinelli LD, Oshry E. Radioactive iodine therapy: effect on functioning metastases of adenocarcinoma of the thyroid. *J Am Med Assoc*. 1946;132:838–847.
2. Silberstein EB, Alavi A, Balon HR, et al. The SNMMI practice guideline for therapy of thyroid disease with 131I 3.0. *J Nucl Med*. 2012;53:1633–1651.
3. Darr AM, Opfermann T, Niksch T, et al. Low-activity 124I-PET/low-dose CT versus 99mTc-pertechnetate planar scintigraphy or 99mTc-pertechnetate

single-photon emission computed tomography of the thyroid: a pilot comparison. *Clin Nucl Med*. 2013;38:770–777.

4. Gulec SA, Kuker RA, Goryawala M, et al. (124)I PET/CT in patients with differentiated thyroid cancer: clinical and quantitative image analysis. *Thyroid*. 2016;26:441–448.
5. Phan HT, Jager PL, Paans AM, et al. The diagnostic value of 124I-PET in patients with differentiated thyroid cancer. *Eur J Nucl Med Mol Imaging*. 2008;35:958–965.
6. Johansson L, Mattsson S, Nosslin B, et al. Effective dose from radiopharmaceuticals. *Eur J Nucl Med*. 1992;19:933–938.
7. Pentlow KS, Graham MC, Lambrecht RM, et al. Quantitative imaging of iodine-124 with PET. *J Nucl Med*. 1996;37:1557–1562.
8. Knust EJ, Dutschka K, Weinreich R. Preparation of 124I solutions after thermodistillation of irradiated 124TeO2 targets. *Appl Radiat Isot*. 2000; 52:181–184.
9. Schmitz J. The production of [124I]iodine and [86Y]yttrium. *Eur J Nucl Med Mol Imaging*. 2011;38 Suppl 1:S4–S9.
10. Jentzen W, Hobbs RF, Stahl A, et al. Pre-therapeutic (124)I PET(/CT) dosimetry confirms low average absorbed doses per administered (131)I activity to the salivary glands in radioiodine therapy of differentiated thyroid cancer. *Eur J Nucl Med Mol Imaging*. 2010;37:884–895.
11. Nagarajah J, Jentzen W, Hartung V, et al. Diagnosis and dosimetry in differentiated thyroid carcinoma using 124I PET: comparison of PET/MRI vs PET/CT of the neck. *Eur J Nucl Med Mol Imaging*. 2011;38: 1862–1868.
12. Jentzen W, Weise R, Kupferschlager J, et al. Iodine-124 PET dosimetry in differentiated thyroid cancer: recovery coefficient in 2D and 3D modes for PET(/CT) systems. *Eur J Nucl Med Mol Imaging*. 2008;35:611–623.
13. O'Doherty J, Jauregui-Osoro M, Brothwood T, et al. ^{18}F-Tetrafluoroborate, a PET probe for imaging sodium/iodide symporter expression: whole-body biodistribution, safety, and radiation dosimetry in thyroid cancer patients. *J Nucl Med*. 2017;58:1666–1671.
14. Lamparter D, Boschi F, Malinconico M, et al. Improved production of iodine-124 for clinical and preclinical applications. *J Label Compd Rad*. 2017;60:S595.
15. Jauregui-Osoro M, Sunassee K, Weeks AJ, et al. Synthesis and biological evaluation of [(18)F]tetrafluoroborate: a PET imaging agent for thyroid disease and reporter gene imaging of the sodium/iodide symporter. *Eur J Nucl Med Mol Imaging*. 2010;37:2108–2116.
16. Binse I, Poeppel TD, Ruhlmann M, et al. Imaging with (124)I in differentiated thyroid carcinoma: is PET/MRI superior to PET/CT? *Eur J Nucl Med Mol Imaging*. 2016;43:1011–1017.
17. Ruhlmann M, Jentzen W, Ruhlmann V, et al. High level of agreement between pretherapeutic 124I PET and intratherapeutic 131I imaging in detecting iodine-positive thyroid cancer metastases. *J Nucl Med*. 2016;57: 1339–1342.